Limnol. Oceanogr., 50(3), 2005, 872–882

A general kinetic model for iron acquisition by eukaryotic phytoplankton

Yeala Shaked,[1] *Adam B. Kustka, and François M. M. Morel*
Geosciences Department, Princeton University, Princeton, New Jersey 08544

Abstract

The conventional model of iron uptake in marine eukaryotic phytoplankton—the Fe′ model—suggests a dependency of uptake rate on the concentration of unchelated iron species (Fe′), and not the concentration of total iron or iron chelated with organic ligands. However, iron in seawater is bound by strong organic ligands that buffer such low Fe′ concentrations that they should not support phytoplankton growth. Studies that show uptake and extracellular reduction of siderophore-bound iron by diatoms and provide indications that the iron uptake system of phytoplankton may be similar to that of yeast in which extracellular reduction is a prerequisite for uptake, call for revisions of the Fe′ model. In this paper we propose a new model for iron uptake by diatoms in which extracellular reduction of all Fe species is a necessary step for iron acquisition. Experiments verifying the predictions of the model are presented. In particular we show data supporting the fact that Fe(II) is formed as an intermediate during Fe uptake from all experimental media, including those buffered by Fe(III)EDTA. This model reconciles the standing Fe′ model with new data and concepts on reduction of iron chelates and provides a convenient framework for designing and interpreting iron uptake experiments in a variety of natural and artificial media.

A major role for iron in marine phytoplankton physiology, ecosystem structure, and the ocean carbon cycle is emerging from numerous oceanographic studies (e.g., Wells et al. 1994; Maldonado et al. 2001). Trace metal clean procedures and many innovative analytical techniques have provided accurate measurements of oceanic iron concentrations and are beginning to reveal the speciation and cycling of iron in the ocean (e.g., Johnson et al. 1997; Rue and Bruland 1997). In order to understand the import of these findings for phytoplankton physiology and ecology, we must understand the relationship between uptake mechanisms of phytoplankton and the concentration and speciation of iron in seawater. The conventional model of iron uptake by marine eukaryotic phytoplankton—the Fe′ model—suggests a dependency of uptake rate on the concentration of unchelated Fe species (Fe′) (Hudson and Morel 1990, 1993; Sunda and Huntsman 1995). According to this model, Fe is acquired via binding of Fe(III)′ or Fe(II)′ to a surface ligand and subsequent internalization by transfer across the plasma membrane (Fig. 1a). The rate of uptake is hence controlled by the rate of ligand exchange between the iron species and a membrane transporter (Hudson and Morel 1990). The Fe′ model is a kinetic extension of the earlier free Fe^{3+} model, a ''quasi-equilibrium'' model in which the extent of binding of Fe to transport ligands and thus the Fe uptake rate were taken to be proportional to the activity of Fe^{3+} (Anderson and Morel 1982). The Fe′ model along with the general free metal ion model have been successfully applied to laboratory studies of trace metal algal physiology and toxicity studies over the last 25 years (e.g., Sunda and Guillard 1976; Anderson et al. 1978; Brand et al. 1983). In a well-buffered medium containing a large excess of aminocarboxylate chelating agents, such as EDTA (ethylenediaminetetraacetic acid), CDTA (cyclohexanediaminetetra acetic acid), NTA (nitrilotriacetic acid), and DPTA (diethylenetriaminepentaacetic acid), Fe(III) is predominantly found in a 1:1 complex with the chelating agent (Y). The unchelated Fe concentration, Fe′ (=Fe(III)′), is maintained by the formation and dissociation of the complex FeY, which is present at 100–1,000 times higher concentrations. The value of Fe′ is determined by the total Fe concentration and the total concentration and the Fe(III) affinity of the chelating agent Y. In addition, for Fe(III) chelates that are photoreactive, Fe′ depends on the light intensity that controls the rate of photochemical FeY degradation (Fe′ = Fe(III)′ + Fe(II)′; Fig. 1a). Variations in Fe′ concentrations obtained by adjusting these parameters have been found to yield proportional variations in the rate of Fe uptake, thus providing a robust experimental support for the Fe′ model (e.g., Hudson and Morel 1990; Sunda et al. 1991; Sunda and Huntsman 1997).

Despite the prevalence of experimental data supporting it, the Fe′ model is now in doubt. Electrochemical measurements have shown that most of the iron in seawater is bound by strong organic ligands that buffer such low Fe′ concentrations that they should not support phytoplankton growth (Gledhill and van Den Berg 1994; Rue and Bruland 1995; Wu and Luther 1995). Laboratory studies have also shown that phytoplankton cultures can obtain Fe and grow in the presence of the model siderophores desferrioxamine B and O, which, like the oceanic strong ligands, maintain very low Fe′ concentrations (e.g., Allnutt and Bonner 1987*b*; Soria-Dengg and Horstmann 1995; Maldonado and Price 2000). Using strong Fe(II) complexing agents, these studies have also shown that Fe(III) may be reduced in culture medium and that addition of Fe(II) chelators inhibits uptake. It has thus been proposed that uptake of Fe(III) from siderophores involves a reduction step (e.g., Allnutt and Bonner 1987*b*; Keshtacher et al. 1999; Maldonado and Price 2001). Additionally, previous reports of diatom mediated reduction in the FeEDTA system suggest that it may be a prevalent strategy for Fe acquisition from other Fe species (Anderson and Morel 1980; Jones et al. 1987). Extracellular reduction of Fe

[1] Corresponding author (yshaked@princeton.edu).

Acknowledgments

This work was partially supported by the Center for Environmental Bioinorganic Chemistry funded by NSF. Y.S. wishes to thank the ISF Bikura Fellowship for financial support.

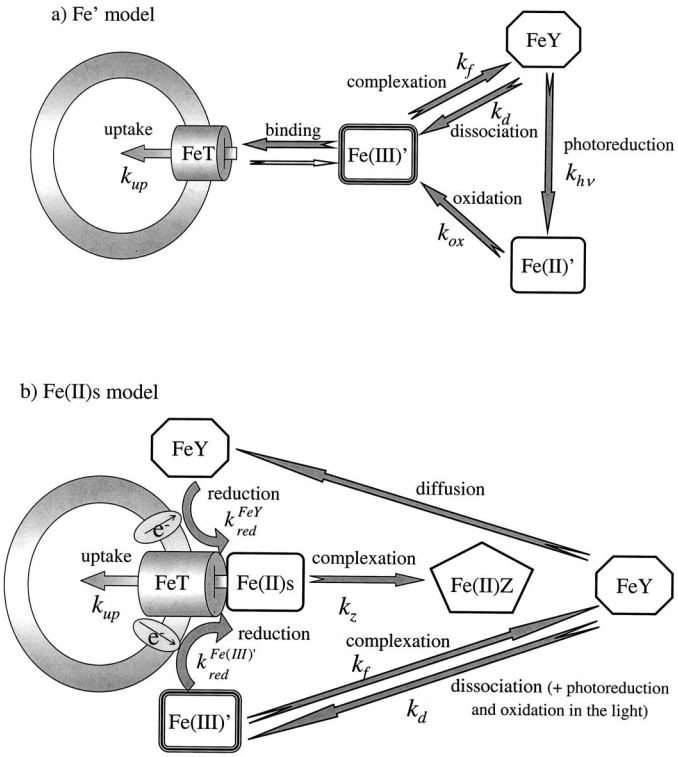

Fig. 1. Schematic illustrations of the (a) Fe′ and (b) Fe(II)s models. (a) In medium buffered by large excess of chelating agent Y, unchelated Fe(III) (Fe′) is maintained at chemical equilibrium with the chelate FeY through dissociation (rate constant k_d) and complexation (rate constant k_f) reactions. Upon illumination, photoreduction of photolabile FeY generates unchelated reduced iron, Fe(II)′, which is rapidly oxidized to Fe(III)′. Fe(III)′ is the dominant species that binds to cell surface ligand (FeT) and is being transported across the cell membrane. The rate of uptake is proportional to Fe(III)′ concentrations (rate constant k_{up}). (b) Fe(III) in both unchelated (Fe(III)′) and chelated (FeY) forms is reduced by surface reductases to form reduced iron at the cell surface, Fe(II)s. Fe(II)s is a transient species that can be either transported across the cell membrane (probably following oxidation) or complexed by ligand in the medium (Z). The uptake rate is proportional to the Fe(II)s concentration (rate constant k_{up}).

is a common Fe acquisition strategy in higher plants (strategy I, Beinfait 1987) and fungi (Askwith and Kaplan 1997). Detailed studies of Fe uptake in the baker's yeast *Saccharomyces cerevisiae* have revealed a complex mechanism of high affinity Fe acquisition that involves two consecutive redox transformations of the Fe. First Fe(III) is reduced to Fe(II) by plasma membrane reductases (Fre1p and Fre2p); then Fe is taken up by an inducible protein complex containing a multicopper oxidase (Fet3p), which oxidizes Fe(II) back to Fe(III), and an iron permease (Ftr1p), which transports Fe(III) across the cell membrane (Eide 1998; Van Ho et al. 2002). Genes homologous to those that encode for these proteins have been identified in the recently sequenced genome of the diatom *Thalassiosira pseudonana* (Armbrust et al. 2004). In addition to the previously mentioned extracellular reduction by diatoms, recent data have shown the involvement of Cu in the Fe uptake process of *Thalassiosira pseudonana,* presumably via a multicopper oxidase (Maldonado pers. comm.)

In this study, we formulate a new kinetic model for Fe acquisition by diatoms and possibly other eukaryotic algae based on all published observations. Based on the model we generate a series of predictions regarding the rates of Fe reduction and uptake under different conditions and examine them in a series of experiments with *Thalassiosira pseudonana* and *Thalassiosira weissflogii.* Those experimental results are then further used to constrain the model parameters. We use the model to reproduce other published data and discuss its implications.

Methods

Culturing—The centric diatoms *Thalassiosira weissflogii* (CCMP 1336) and *Thalassiosira pseudonana* (CCMP 1335) were grown in polycarbonate bottles under Fe-limited conditions (60 nmol L^{-1} and 100 nmol L^{-1} Fe, respectively, with 100 μmol L^{-1} EDTA) at 20°C under continuous light (80–100 μmol quanta m^{-2} s^{-1}). We chose to work with *T. weissflogii* to allow direct comparison with previous kinetic studies (e.g., Anderson and Morel 1982; Hudson and Morel 1990; Sunda and Huntsman 1995), and *T. pseudonana* to allow future complementary studies based on its recently published genome (Armbrust et al. 2004). The experimental medium was prepared from 0.2-μm filtered Gulf Stream water enriched with chelexed major nutrients (10 μmol L^{-1} PO_4^{3-}, 100 μmol L^{-1} NO_3^-, and 100 μmol L^{-1} SiO_2), filter sterilized vitamins, and trace metals (40 nmol L^{-1} Cu, 50 nmol L^{-1} Mn, 100 nmol L^{-1} Zn, and 40 nmol L^{-1} Co) buffered with 100 μmol L^{-1} EDTA to approximate the free ion activities found in seawater. Cells were counted using a Multisizer II Coulter Counter, and specific growth rates were then determined from the linear regressions of the natural log of cell density versus time. Sterile trace metal clean techniques were applied for culturing and experimental manipulations. Solutions were prepared with double-distilled water (Milli-Q, Millipore, 18.2 mΩ), analytical or ultrapure acids and bases, and analytical or higher grade salts.

Simultaneous Fe reduction and uptake determination in the FeEDTA system—The method applied in this study is based on the addition of the cell impermeable specific Fe(II)-binding ligand ferrozine (FZ, 3-(2-pyridyl)-5,6-bis(4-phenylsulphonic acid)-1,2,4-triazine) to seawater with radiolabeled Fe(III)EDTA. The rate of iron uptake is determined simultaneously with the rate of Fe(II) binding to FZ, measured by the retention of the $Fe(II)FZ_3$ complex on C_{18} Sep-Pak columns. A complete description of the method can be found in Shaked et al. (2004). Briefly, $^{59}FeCl_3$ (Perkin Elmer) was precomplexed with EDTA at a ratio of 1 : 1.1 prior to the experiments and applied at a specific activity of 1–7 $\times$ 10^{16} Bq mol Fe^{-1}. The pH of the experimental medium and the ^{59}FeEDTA stock were adjusted to pH 8.0 and the solutions were equilibrated in the dark overnight. The concentrations of Fe and EDTA used in different experiments ranged between 20 and 115 nmol L^{-1} Fe and 5 and 2,000 μmol L^{-1} EDTA. *Thalassiosira* spp. do not require light to acquire Fe (Anderson and Morel 1982; Hudson and Morel 1990); thus,

all short-term experiments were conducted in the dark. Exponentially growing cells were filtered, rinsed twice with Aquil medium (Price et al. 1988/89), and resuspended, and aliquots were dispensed to different polycarbonate bottles with experimental medium. FZ was added to some of the treatments at 100–300 μmol L^{-1}. Previously, we verified that FZ had no adverse effect on the photosynthetic capacity of the cells by measuring the ratio of variable to maximum fluorescence (Fv : Fm) with DCMU (dichlorophenyldimethyl urea) (Shaked et al. 2004). In this study we additionally confirmed that FZ, at the concentrations of interest, does not influence cellular carbon assimilation (using ^{14}C) throughout the 3–6 h of short-term uptake experiments. At discrete time points, 15–40-ml aliquots from each treatment were removed and loaded using a four head peristaltic pump on prewetted 0.8-μm syringe filters (13 mm, Versapor). Sep-Pak C_{18} columns located downstream from the filters were used to retain the $^{59}Fe(II)FZ_3$. The filters were placed on a second peristaltic pump, washed first with pH 8 NaCl (0.5 mol L^{-1} NaCl, 5 mmol L^{-1} $NaHCO_3^-$), and then washed for 2 min with Ti-citrate-EDTA solution to remove adsorbed extracellular Fe (Hudson and Morel 1989). The filters were washed again for 2 min with pH 8 NaCl, followed by a rinse of the filter housing. Meanwhile, the Sep-Pak columns, left in their original position, were washed with pH 2 NaCl (0.5 mol L^{-1} NaCl, 5 mmol L^{-1} HCl) for 5 min to remove any adsorbed Fe(III) species from the column. After purging the retention volume of pH 2 NaCl from the Sep-Pak, the $Fe(II)FZ_3$ complex was eluted from the column by methanol. The ^{59}Fe in the syringe filters and the methanol effluent was counted on a 1480 Wizard 3″ gamma counter.

FeDFB uptake experiments and Fe′ calculations—The fungal siderophore desferrioxamine B (DFB, a term which applies to the deferrated ligand only but would be used here to describe the complexed form as well) was purchased from Sigma and dissolved in Milli-Q water. Stock solutions of $^{59}FeDFB$ were made at pH 5–6 with a Fe : DFB ratio of 1 : 1.1. $^{59}FeDFB$ was added to Aquil (Price et al. 1988/89) without added trace metals (to maintain EDTA free conditions) or 0.2-μm filtered Gulf Stream seawater and was allowed to equilibrate overnight. The specific Fe(II) ligand bathophenanthroline disulphonic acid (BPDS, Sigma) was used in several uptake experiments in addition to FZ.

Constants used for Fe′ calculations in FeEDTA-buffered media are effective constants (i.e., take into account the interactions of EDTA with Ca and Mg) from Hudson et al. (1992) and Sunda and Huntsman (2003). A stability constant ($K^{cond}_{Fe'L}$, Fe′) of $10^{16.5}$ $(mol\ L^{-1})^{-1}$ was used to calculate Fe′ in FeDFB buffered medium (Hudson et al. 1992).

The Fe(II)s model—We base our new model on the hypothesis that the Fe uptake mechanism in eukaryotic algae is akin to that of yeast and involves a reduction of Fe(III) at the surface prior to transport across the membrane, which presumably involves a reoxidation of Fe(II). We do not attempt to represent in the model all individual molecular steps but aim at describing the essential features of the uptake mechanism using the smallest number of variables. The conceptual basis of the new Fe(II)s model is illustrated in Fig. 1b and contrasted with the Fe′ model in Fig. 1a.

To explicitly include the necessary reduction step, it is convenient to define a concentration of Fe(II) at the surface, [Fe(II)s], which determines the rate of uptake by the cell (Fig. 1b).

$$\text{uptake}(\rho) = k_{up}[\text{Fe(II)s}] \quad (1)$$

where the uptake rate is in units of mol $cell^{-1}$ h^{-1}; Fe(II)s is in mol $cell^{-1}$; k_{up} is the rate constant of Fe internalization by the membrane transporters under nonsaturating Fe(III)′ concentrations and it has units of h^{-1}. The magnitude of k_{up} depends on the preconditioning of the cells, which determines whether the cells regulate up or down the number of transporters on the membrane. The formation of Fe(II)s results from the reduction of Fe(III) at the cell surface. In order to reconcile previous data on Fe(III)′ uptake and Fe-siderophore uptake we assume that both the unchelated Fe, Fe(III)′, and the chelate FeY can be reduced. Because this extracellular Fe reduction has been commonly quantified using nonpermeable specific Fe(II) chelating agents (such as FZ and BPDS), it appears that the cell-generated Fe(II)s is accessible by Fe(II) ligands in the medium. The concentration of Fe(II)s is thus determined by the balance of four processes: cell surface reduction of FeY, cell surface reduction of Fe(III)′, complexation of Fe(II)s by some ligand Z present in the medium, and uptake of Fe(II)s by the cells (Fig. 1b). The corresponding differential equation can be written

$$\frac{d[\text{Fe(II)s}]}{dt} = k^{FeY}_{red}(\text{FeY}) + k^{Fe(III)'}_{red}[\text{Fe(III)}'] - k_z[\text{Fe(II)s}][\text{Z}] - k_{up}[\text{Fe(II)s}] \quad [2]$$

where k^{FeY}_{red} and $k^{Fe(III)'}_{red}$ are kinetic constants for cell surface reduction of FeY and Fe(III)′, respectively, in units of L $cell^{-1}$ h^{-1}; and k_z is the formation constant for the $Fe(II)Z_n$ complex in units of $(mol\ L^{-1})^{-1}$ h^{-1}. The ligand Z represents any potential Fe(II) ligand in the medium, including the one used to chelate Fe(III) (then Z = Y). Obviously more than one such complexing agent could be considered in the model. We shall specifically consider the Fe(II) ligands FZ and BPDS as well as DFB and EDTA as potential competitors with cellular uptake for Fe(II)s. We did not include the reoxidation of Fe(II)s by oxygen in this model. Oxygen, pH, and other parameters that might affect the reoxidation of Fe(II)s were kept constant in ours and other published experiments, and hence reoxidation of Fe(II)s was considered implicitly as part of the efficiency of the surface reduction.

When there is no photoreduction of the FeY complex (all the experiments were performed in the dark), the concentration of Fe(III)′ in the medium is determined by three processes: dissociation of Fe(III)′ from the FeY complex, complexation of Fe(III)′ by the chelating agent Y, and reduction of Fe(III)′ by the cells (Fig. 1b), as embodied in the following equation

$$\frac{d[\text{Fe(III)}']}{dt} = k_d(\text{FeY}) - k_f[\text{Fe(III)}'][\text{Y}] - k^{Fe(III)'}_{red}N[\text{Fe(III)}'] \quad (3)$$

where k_d is the thermal dissociation constant of the FeY complex in units of h^{-1}; k_f is the effective formation constant of the FeY complex in units of $(\text{mol L}^{-1})^{-1}\ h^{-1}$, and N is the number of cells in 1 liter of medium.

At steady state ($d[\text{Fe(II)s}]/dt = d[\text{Fe(III)}']/dt = 0$), we can derive an expression for [Fe(III)′] and [Fe(II)s] and combine them to obtain an equation for the rate of cellular uptake (in units of mol Fe $\text{cell}^{-1}\ h^{-1}$)

$$\text{uptake } (\rho) = \frac{\left[k_{\text{red}}^{\text{FeY}} + \dfrac{k_{\text{red}}^{\text{Fe(III)}'} k_d}{k_f[\text{Y}] + k_{\text{red}}^{\text{Fe(III)}'} N}\right][\text{FeY}]}{\dfrac{k_z[\text{Z}]}{k_{\text{up}}} + 1} \quad (4)$$

Note that the values and units of k_{up} in this model are different from those of the Fe′ model, where k_{up} of the Fe′ model (in units of L $\text{cell}^{-1}\ h^{-1}$) is essentially similar to $k_{\text{red}}^{\text{Fe(III)}'}$ in the Fe(II)s model, while k_{up} in the Fe(II)s model (in units of h^{-1}) describes the transport of a cell surface species Fe(II)s (in units of mol Fe cell^{-1}). To discuss the role of the various terms, we can define three parameters *A*, *B*, and *C* for the simplified expression

$$\text{uptake } (\rho) = \frac{(A + B)[\text{FeY}]}{C + 1} \quad (5)$$

A represents the contribution of the surface reduction of the chelate FeY to the uptake, while *B* represents the contribution of the surface reduction of Fe(III)′. In the case of an FeEDTA-buffered system (Y = EDTA), *B* must predominate over *A* so that the model is consistent with the Fe(III)′ model. In contrast, if Y is a siderophore Fe(III)′ is extremely small and *A* must predominate over *B*. *C* represents the competition for Fe(II)s between the cells and the free ligand in the medium.

Results

As described, the Fe(II)s model is formulated a priori based on published observations. Its distinguishing features are that all sources of Fe must be reduced at the surface prior to uptake and that Fe(III)′ itself is a substrate for that reduction. The first sets of experiments described below were designed to support these two postulates. To further buttress the validity of the model, we performed other experiments designed to test some of the model predictions under particular experimental conditions.

Effects of specific Fe(II) ligands—To demonstrate cellular reduction of Fe(III), previous studies have used the Fe(II) specific ligands FZ and BPDS that produce a complex that is measurable spectrophotometrically (Anderson and Morel 1980; Maldonado and Price 1996; Shaked et al. 2002). Because of the low detection limit of the method, these experiments were conducted using high concentrations of Fe and chelating agents to produce nanomolar to micromolar concentrations of Fe(II) complex that could be measured. Such experiments are thus subject to the criticism that BPDS or FZ themselves may promote the reduction of Fe(III). More importantly, it is uncertain that these experiments can be simply extrapolated to conditions of low Fe concentrations where only nanomolar or lesser Fe concentrations are taken up and hence presumably reduced at the surface of the cells. We used a method that combines radiometric detection with Fe(II) separation onto columns to simultaneously measure cellular uptake and FZ binding of Fe(II) at subnanomolar levels in FeEDTA-buffered medium (Shaked et al. 2004). The method has been found to be free of major experimental artifacts and to yield reproducible linear rates for short-term experiments (3–6 h). We have not conducted Fe reduction measurements in the presence of FeDFB because it adsorbs to the C_{18} columns used to separate the $^{59}\text{Fe(II)FZ}_3$. Extracellular reduction of FeDFB and its role in Fe acquisition by diatoms is, however, relatively well documented (Allnutt and Bonner 1987*a*; Soria-Dengg and Horstmann 1995; Maldonado and Price 2001).

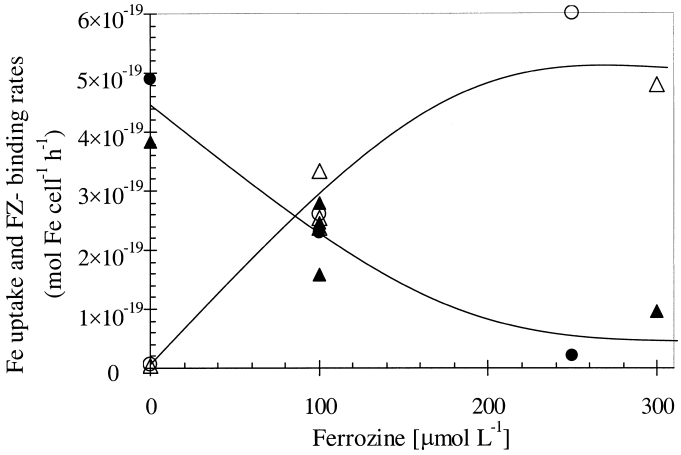

Fig. 2. Simultaneously determined Fe uptake (filled symbols) and Fe reduction (=FZ binding; open symbols) rates in Fe-limited *T. weissflogii* cultures (2.4×10^5 cell ml^{-1}) as a function of FZ concentration. Short-term experiments were conducted in Aquil medium containing 90 nmol L^{-1} Fe and 100 μmol L^{-1} EDTA in the dark. The triangles and circles represent rates from two different experiments.

A typical set of experiments in which short-term Fe reduction (=FZ binding) and uptake rates by Fe-limited *T. weissflogii* (in the presence of 90 nmol L^{-1} Fe, 100 μmol L^{-1} EDTA, and 0–300 μmol L^{-1} FZ) were determined simultaneously is shown in Fig. 2. Increasing the FZ concentration resulted in elevated FZ binding rates and inhibited uptake rates, while the sum of both processes remained roughly constant over this range of FZ concentrations (Fig. 2). This behavior is characteristic of competition for Fe(II) between the cells and FZ. At first we interpreted the quantitative agreement between the inhibitory effect of FZ on uptake rate and the rate of Fe(II) captured by FZ (Fig. 2) as a firm demonstration that reduction of all Fe(III) species is a necessary step in Fe uptake. We found, however, that this quantitative relationship did not always hold. A significant fraction of the reduction measured in our experiments occurs in the bulk medium, some by reaction with superoxide (O_2^-), which is formed in *T. weissflogii* medium (Kustka et al. in press). Because of rapid reoxidation in the medium (in the absence of FZ), the corresponding production of Fe(II) re-

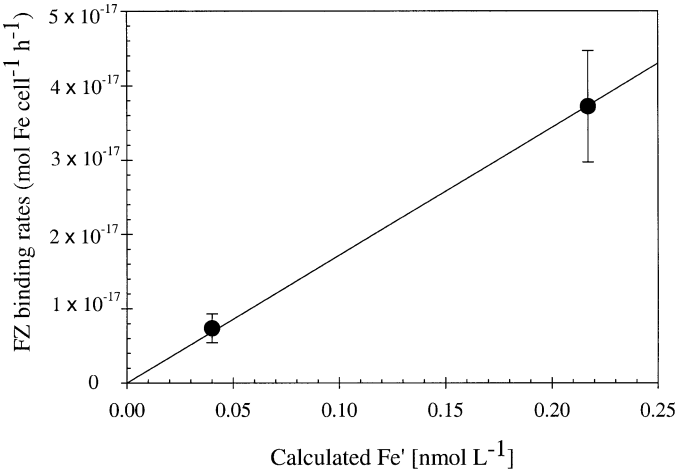

Fig. 3. Fe reduction rate (=FZ binding) by Fe-limited *T. weissflogii* (3.5×10^4 cell ml^{-1}) as a function of calculated Fe(III)′ concentrations. Experiments were conducted in the dark in Aquil medium containing 115 nmol L^{-1} Fe and 20 or 100 μmol L^{-1} EDTA at pH = 8.00 ± 0.05. FZ binding rates were calculated from the linear regression of four time points over the 4 h of the experiments. Vertical error bars represent the error around the slope. Fe(III)′ concentrations were calculated for pH = 8.0 using the effective constants of Sunda and Huntsman (2003).

sults in no measurable change in Fe(III)′ or uptake rate. It is of course likely that reduction of Fe(III) in the bulk medium, some or most of which may be mediated by O_2^- (Kustka et al. 2005), affected, and perhaps dominated, many of the previous studies of Fe(II) formation in diatom cultures. For our purpose, the quantitative agreement between measured reduction rates and uptake inhibition should be considered fortuitous. Thus the data in Fig. 2 demonstrating simultaneous reduction and uptake of Fe in FeEDTA-buffered systems provide only strong qualitative support for the Fe(II)s model.

Fe reduction is modulated by Fe(III)′—The Fe(II)s model is constructed to account for the rate of uptake from both chelated and unchelated Fe. In an EDTA-buffered medium maintained in the dark, Fe is present at significant concentrations in both forms, Fe(III)′ and FeEDTA. As mentioned before, the Fe′ model, which has been validated for the FeEDTA system, predicts a proportionality between Fe(III)′ concentrations and uptake rate. The Fe(II)s model will generate similar prediction if Fe(III)′ is the major species that is being reduced by the cells. In order to examine whether FeEDTA or Fe(III)′ is being reduced, we conducted two parallel experiments with constant Fe (115 nmol L^{-1}) but variable EDTA (20 μmol L^{-1} and 100 μmol L^{-1}) at pH 8 ± 0.05, resulting in a fivefold decrease in Fe(III)′ from 0.22 nmol L^{-1} at the 20 μmol L^{-1} EDTA treatment to 0.04 nmol L^{-1} at the 100 μmol L^{-1} EDTA treatment (Fig. 3). The reduction rate measured for Fe-limited *T. weissflogii* in the presence of 100 μmol L^{-1} FZ was found to vary fivefold, proportionally to the change in Fe(III)′ concentrations (Fig. 3). Thus Fe(III)′ is the principal species being reduced by the cells. This conclusion is not affected by the fact that a significant fraction of the measured Fe(III) reduction rate is occurring in the bulk medium (Kustka et al. in press).

The experiments shown in Figs. 2 and 3, and similar ones, provide an estimate of the cellular rate constant for Fe(III)′ reduction ($k_{red}^{Fe(III)'}$). As shown later, in FeEDTA systems buffered by EDTA concentrations in the range of 5–100 μmol L^{-1}, Fe(III)′ reduction dominates over FeEDTA reduction ($B \gg A$ in Eq. 5), and EDTA does not compete effectively with the cells for Fe(II)s ($C \ll 1$). For experiments conducted at low cell density (N), we can neglect $k_{red}^{Fe(III)'}N$. The simplified expression for uptake (Eq. 4) can then be written as

$$\rho = k_{red}^{Fe(III)'} \times [Fe(III)'] \quad (6)$$

and we can calculate $k_{red}^{Fe(III)'}$ for each uptake experiment. The measured value of $k_{red}^{Fe(III)'}$ varied between 5×10^{-9} and 9×10^{-8} L cell^{-1} h^{-1} in different experiments with *T. weissflogii* depending on the cells preconditioning (similarly to k_{up} in the Fe(III)′ model, Table 1). For each set of measurements performed with a single batch of cells, however, $k_{red}^{Fe(III)'}$ remained constant for all treatments. Somewhat lower $k_{red}^{Fe(III)'}$ values of ~5–7 $\times 10^{-9}$ L cell^{-1} h^{-1} were found for *T. pseudonana* in accordance with its smaller cell size. In general, $k_{red}^{Fe(III)'}$ is well constrained as observed from the values in Table 1, calculated from uptake experiments with different microalgae.

Upper limit for the rate of Fe uptake in FeEDTA system—The maximal rate of uptake according to the Fe′ model is the rate of Fe(III) supplied by FeEDTA dissociation. This limit should be approached experimentally at high cell concentrations and low total Fe concentration. (In those usually undesirable experimental conditions, the FeEDTA buffer is ''blown'' because the rate of Fe uptake by the whole culture approaches the rate of the chemical reactions and the steady state Fe(III)′ concentration becomes controlled partly by the total rate of cellular uptake.) Because the supply of Fe(III)′ by dissociation of FeEDTA is limited, these conditions are also most suitable to test the importance of FeEDTA reduction to supply Fe to the cells. If Fe(III)′ is the major species reduced by the cells, the total uptake rate is expected to reach a maximum defined by the FeEDTA dissociation rate as the cell concentration increases. If the cells are able to reduce the abundant FeEDTA at a significant rate, the uptake rate is expected to exceed the rate of FeEDTA dissociation and to keep increasing as the cell concentration increases. Mathematically, C in Eq. 5 and k_f[Y] in B can be neglected. The total rate of uptake in the culture (ρN in units of mol L^{-1} h^{-1}) is then determined by the sum of FeEDTA dissociation and FeEDTA reduction

$$\text{Total} - \text{uptake}(\rho N) = (k_{red}^{FeY}N + k_d)[FeY] \quad (7)$$

We conducted two sets of uptake experiments at increasing *T. weissflogii* cell concentrations using 20 nmol L^{-1} Fe and 20 μmol L^{-1} EDTA (Fig. 4). The relatively low EDTA was chosen to allow initial high Fe(III)′ and hence fast Fe acquisition, while the low total Fe was chosen to maintain slow FeEDTA dissociation rate. The first time point of the uptake experiment was taken about an hour after the cell addition to the experimental medium to allow the cells to consume the initial Fe(III)′ fixed by the chelating agent and a new

Table 1. Fe(II)s model parameters. Values are calculated from current and published uptake rates or evaluated by model fit to experimental data.

Parameters (units)	Ligand/complex	Value: Lower limit	Value: Upper limit	Experimental conditions/organism data source
k_d	Dissociation constant of Fe(III) from FeY complex			
(h^{-1})	EDTA	4.0×10^{-4}		pH 8, effective constant*†
k_f	Effective formation constant of FeY complex			
(mol L^{-1} h^{-1})		7.2×10^{4}		pH 8, effective constant†
$k_{red}^{Fe(III)'}$	Cellular Fe(III)′ reduction constant			
(L $cell^{-1}$ h^{-1})	Fe(III)′	3.0×10^{-8}	9.0×10^{-8}	*T. weissflogii*, variable EDTA exp. (Fig. 6; $n=6$)
	Fe(III)′	4.6×10^{-9}	6.2×10^{-8}	*T. weissflogii*, FeEDTA exp. ($n=9$)
	Fe(III)′	2.0×10^{-8}	4.0×10^{-8}	*T. weissflogii*‡§
	Fe(III)′	5.5×10^{-9}	7.1×10^{-9}	*T. pseudonana*, FeEDTA exp. ($n=4$)
	Fe(III)′	2.0×10^{-9}	4.6×10^{-9}	*T. pseudonana*‡§
	Fe(III)′	5.2×10^{-9}	4.6×10^{-8}	*T. oceanica, T. parteneia, T. subtilis* (diatoms)§
	Fe(III)′	3.2×10^{-9}	1.1×10^{-8}	*E. huxleyi*‡ (coccolithophore)
	Fe(III)′	1.3×10^{-8}	5.7×10^{-8}	*P. minimum*‡ (dinoflagellate)
k_{red}^{FeY}	Cellular FeY reduction constant			
(L $cell^{-1}$ h^{-1})	FeEDTA	5.4×10^{-12}	($\pm5.3\times10^{-12}$)	*T. weissflogii* high cell No. (Fig. 4, $n=7$)
	FeEDTA	0	1.0×10^{-12}	*T. weissflogii* variable EDTA (Fig. 6) model fit
	FeDFB	2.9×10^{-11}		*T. weissflogii* FeDFB exp. (Fig. 5)
	FeDFB	4.9×10^{-13}	7.1×10^{-13}	*T. pseudonana* FeDFB exp. ($n=4$)
	FeDFB	1.5×10^{-12}	6.5×10^{-12}	*T. oceanica* ($n=12$)‖
	Ferrioxamine	1.9×10^{-10}		*T. weissflogii*¶
	Alterobactin A/B	3.3×10^{-11}		*T. weissflogii*¶
	Ferrichrome	1.6×10^{-10}		*T. weissflogii*¶
k_z/k_{up}	Ratio of Fe(II)s complexation by ligand Z (k_z) and Fe(II)s uptake by the cells (k_{up})			
(mol L^{-1})	EDTA	1.2×10^{3}	1.5×10^{4}	*T. weissflogii* variable EDTA (Fig. 6; $n=6$)
	EDTA	7.6×10^{3}		*T. weissflogii* FeFDB+1 mmol L^{-1} EDTA (Fig. 5)
	DFB	1.0×10^{7}		*T. weissflogii* FeDFB+1 μmol L^{-1} DFB (Fig. 5)
	DFB	2.6×10^{5}	1.8×10^{6}	*T. oceanica*‖
	FZ	8.6×10^{11}	1.0×10^{12}	*T. weissflogii* variable [FZ] (Fig. 2)
	BPDS	2.7×10^{11}		*T. weissflogii* FeDFB+300 μmol L^{-1} BPDS

* Sunda and Huntsman (2003).
† Hudson et al. (1992).
‡ Sunda and Huntsman (1995).
§ Maldonado and Price (1996).
‖ Maldonado and Price (2001).
¶ Hutchins et al. (1999*b*).

steady state Fe(III)′, which depends on cellular uptake, to be reached. A pH of 7.93 ± 0.05 (which corresponds to a dissociation rate of 2.6–4.1 × 10^{-11} mol L^{-1} h^{-1}) was measured in the first experiment (Fig. 4. circles), while a pH of 8.15 ± 0.05 (which corresponds to a dissociation rate of 8.1 × 10^{-11} to 1.4 × 10^{-10} mol L^{-1} h^{-1}) was measured at the end of the second experiment (Fig. 4, triangles). The total rate of Fe uptake in the medium (ρN in units of mol L^{-1} h^{-1}) increased with concentrations at the low cell concentrations and leveled off at high cell concentrations (Fig. 4). As expected, the leveling off occurred at a value that is within the range of calculated FeEDTA dissociation (Fig. 4). Those experiments clearly show that Fe(III)′ is the main variable governing the Fe uptake rate. For the Fe(II)s model, these results provide another support that Fe(III)′ is the prime species that is being reduced by the cells. A slight excess in the rate of uptake above the maximum given by FeEDTA dissociation is perhaps observed at the highest cell concentrations (Fig. 4). From Eq. 7 and the excess of uptake above FeEDTA dissociation (Fig. 4) we can obtain a rough first-order estimate for k_{red}^{FeEDTA} of 5 × 10^{-12} L $cell^{-1}$ h^{-1} (±5 × 10^{-12}, n = 7; Table 1). This value has a large uncertainty because of the noise in the experimental data and the uncertainty regarding small shifts in pH, which have a strong effect on FeEDTA dissociation rate.

Effect of large excess of ligand on uptake rate—One of the important features of the Fe(II)s model is the recomplexation of Fe(II)s by ligands in the medium. We have shown above that the specific Fe(II) ligand FZ (or BPDS) can bind Fe(II) and inhibit the rate of uptake. In principle other ligands, such as EDTA or DFB, should also be able to compete with the cells for the Fe(II)s. EDTA, as well as other carboxylic acids and DFB, have similar formation constants (k_f) for hydrated Fe(II) and for hydrated Fe(III), since the water loss rates from the hydrated Fe, which are the rate limiting step, are comparable (Morel and Hering 1993). Here we examine three conditions: (1) a large excess of DFB in an FeDFB buffered system, (2) a large excess of EDTA in

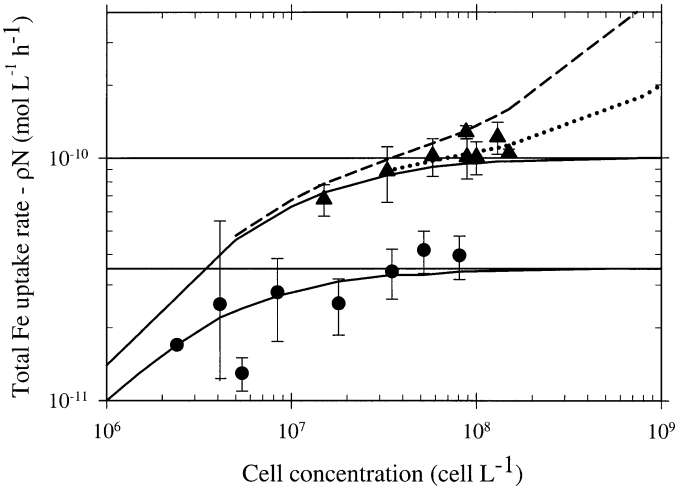

Fig. 4. Total uptake rates (ρN) of Fe-limited *T. weissflogii* as a function cell concentration. Two sets of experiments were conducted in the dark using Aquil medium containing 20 nmol L^{-1} Fe and 20 μmol L^{-1} EDTA, at pH 7.93 ± 0.05 (circles) and 8.15 ± 0.05 (triangles). Solid lines are Fe uptake rates calculated according to Fe′ model, assuming dissociation rates of 3.5×10^{-11} mol L^{-1} h^{-1} (for pH = 7.93) and 1×10^{-10} mol L^{-1} h^{-1} (for pH = 8.15) and k_{up} values of 1.5×10^{-7} L $cell^{-1}$ h^{-1} and 6×10^{-8} L $cell^{-1}$ h^{-1}, respectively. Horizontal lines are calculated FeEDTA dissociation rates for each experiment (not including the pH measurement error). The dotted line is the calculated contribution of FeEDTA reduction by the cells to the total Fe uptake rate, using the average value $k_{red}^{FeY} = 5 \times 10^{-12}$ L $cell^{-1}$ h^{-1}, estimated from this experiment. The dashed line is the upper limit for the contribution of FeEDTA reduction to total Fe uptake rate, calculated using $k_{red}^{FeY} = 2 \times 10^{-11}$ L $cell^{-1}$ h^{-1}.

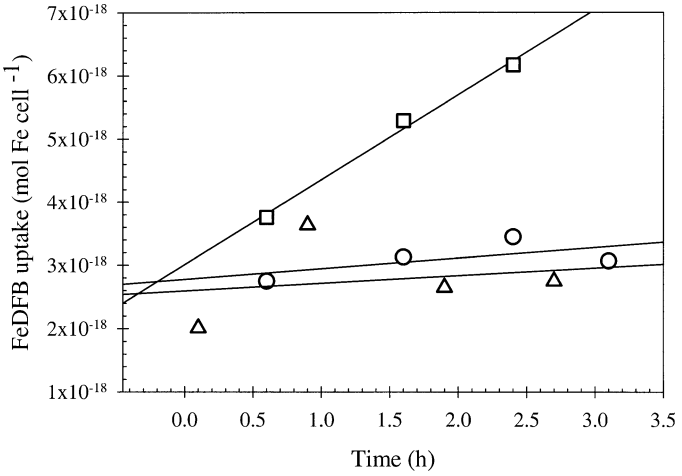

Fig. 5. Short-term FeDFB uptake by Fe-limited *T. weissflogii* (1×10^5 cell ml^{-1}). Experiments were conducted with 45 nmol L^{-1} FeDFB (1 : 1.1 Fe : DFB, squares) and with additions of 1 mmol L^{-1} EDTA (circles) and 1 μmol L^{-1} DFB (triangles). Linear regressions of the experimental observations are drawn.

an FeDFB buffered system, and (3) a large excess of EDTA in an FeEDTA-buffered system.

In an FeDFB buffered system, the reduction of Fe(III)′ should be negligible: $k_{red}^{Fe(III)'} \times Fe(III)' = \sim 1 \times 10^{-8} \times 3 \times 10^{-16} = 3 \times 10^{-24}$ mol $cell^{-1}$ h^{-1}, much below our detection limit. The uptake equation (Eq. 4) can be then simplified and rewritten as

$$\text{uptake } (\rho) = \frac{k_{red}^{FeY}[FeY]}{\frac{k_z[Z]}{k_{up}} + 1} \quad (8)$$

Experiments by Maldonado and Price (2001) have shown that indeed the uptake rate under those conditions is proportional to the concentrations of the FeDFB complex in accord with Eq. 8 (when excess DFB [=Z] is kept constant). From the uptake rate measured in the experiment of Fig. 5, we can calculate a value for k_{red}^{FeDFB} of $\sim 3 \times 10^{-11}$ L $cell^{-1}$ h^{-1} (Table 1). Another calculation from the measured rates of FeDFB uptake by *T. pseudonana* with no excess ligand yields a lower value of ~ 5–7×10^{-13} L $cell^{-1}$ h^{-1} (Table 1, data not shown). These differences between k_{red}^{FeDFB} of the two diatom species are coherent with the differences in $k_{red}^{Fe(III)'}$ (Table 1) and probably reflect mostly the differences in cell size, since their cell surface normalized reduction and uptake rates of FeEDTA and FeDFB are comparable (surface areas of *T. pseudonana* and *T. weissflogii* are 50 μm^2 and 460 μm^2, respectively).

(1) The addition of excess DFB (1 μmol L^{-1}) to the FeDFB medium resulted in significant inhibition of Fe uptake (Fig. 5). Since the reduction and uptake of Fe(III)′ is negligible under these conditions (*see previous paragraph*), the corresponding decrease in Fe(III)′ (from 3×10^{-16} mol L^{-1} to 1×10^{-18} mol L^{-1}) cannot account for the decrease in uptake rate. Thus the inhibition caused by excess DFB cannot be due to a change in speciation of Fe(III) in the medium and indicates clearly that DFB interferes at some intermediate step in the uptake mechanism. In our model, the intermediate step is the formation of Fe(II)s.

(2) An even more dramatic demonstration of the same phenomenon is given by experiments in which high concentrations of EDTA are added to an FeDFB buffered system. A 1 mmol L^{-1} EDTA addition has no effect on Fe(III)′ that is buffered by DFB, or on [FeDFB] itself. Yet, as seen in Fig. 5, this addition of EDTA had a strong inhibitory effect on Fe uptake.

(3) Such an effect of EDTA on Fe uptake, which is independent of its effect on the speciation of Fe[III], should also be observable in an FeEDTA-buffered medium. In Eq. 5, the effect of increasing the EDTA (=Y) concentration on the speciation of Fe (resulting in a lower Fe(III)′) is accounted for by a decrease in the value of parameter B. The other effect of EDTA, that of competing with the cells for Fe(II)s, is accounted for by an increase in parameter *C*. Thus, when EDTA is increased to very high concentrations in the medium, we should see a departure from the Fe(III)′ model when *C* becomes close to and exceeds 1. Under these conditions the uptake rate should be lower than predicted by the Fe′ model.

Barring complications resulting from ligand exchange reactions at the cell surface, EDTA should compete successfully with the cells for Fe(II)s ($C \sim 1$) at similar concentrations in an FeEDTA and an FeDFB buffered system. We,

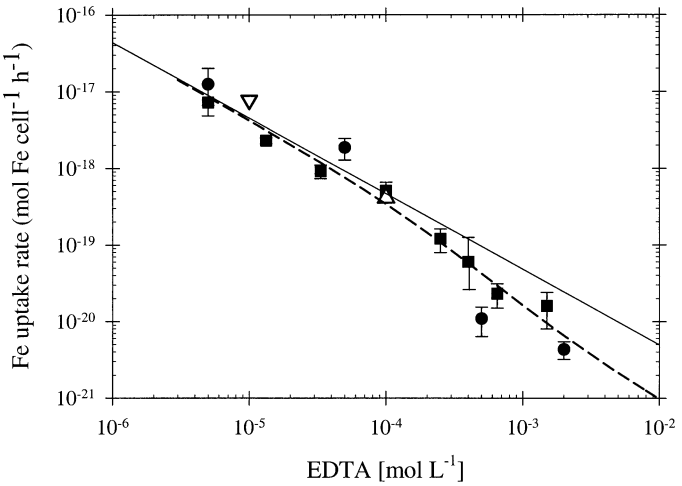

Fig. 6. Short-term uptake rates of Fe-limited *T. weissflogii* as a function of EDTA concentration. Two sets of experimental data measured with 20 nmol L^{-1} Fe are presented (filled circles and squares). The triangle up is an average of uptake experiments measured in this study using 90 nmol L^{-1} Fe ($n = 10$) and the triangle down is average uptake rates measured by Anderson and Morel (1982, $n = 3$), both normalized to 20 nmol L^{-1} Fe. The solid line is calculated uptake rates using the Fe′ model at low cell concentrations (1,000 cell ml^{-1}) and $k_{up} = 4.8 \times 10^{-8}$ L $cell^{-1}$ h^{-1} (Hudson and Morel 1990). The dashed line is calculated uptake rates using the Fe(II)s model and the actual cell concentration in each experiment.

thus, varied the EDTA concentrations from 5 μmol L^{-1} to 2 mmol L^{-1} in two different experiments with Fe-limited *T. weissflogii* cultures in radiolabeled medium containing 20 nmol L^{-1} Fe at pH 8. The cell density was lowered to 2,000 cells ml^{-1} in the experiments with the lowest EDTA concentrations to keep the total rate of uptake low relative to the FeEDTA dissociation rate. High EDTA concentrations from 400 μmol L^{-1} to 2 mmol L^{-1} buffer low Fe(III)′ from 2×10^{-12} mol L^{-1} to 4×10^{-13} mol L^{-1}, so that high cell densities of 2×10^5 cell ml^{-1} were required to obtain a measurable signal.

A deviation from the Fe′ model (depicted in Fig. 6 as the straight line) clearly occurs when the EDTA concentration approaches or exceeds 1 mmol L^{-1}. In that range, the uptake rate is 2–10 times lower than expected from the Fe′ model. This is accounted for in the Fe(II)s model by adjusting the parameter k_z/k_{up}. The fit of the model to the data with $k_z/k_{up} = 2.4 \times 10^3$ mol^{-1} L is shown by the dashed line. A change in the value of that parameter is expected among cultures that have different preconditioning histories and regulate the parameter k_{up} at different values.

We note that a departure from the Fe′ model may have also been caused at high EDTA concentration by the reduction of FeEDTA at the cell surface. In Eq. 5 when B becomes small enough, A may become the dominant term in the numerator, and the uptake rate should be higher than predicted by the Fe′ model. Clearly the data of Fig. 6 indicate that the competition of EDTA with the cells for Fe(II)s (term C in Eq. 5) is dominant over this other effect. A negligible rate of reduction of FeEDTA at the cell surface is consistent with the data. Nonetheless, a value of $k_{red}^{FeEDTA} \sim 1 \times 10^{-12}$ L $cell^{-1}$ h^{-1}, which is within the range of values estimated from the experiments at high cell concentration ($0–2 \times 10^{-11}$ L $cell^{-1}$ h^{-1}, Table 1), slightly improves the fit of the model to the data of Fig. 6.

Discussion

The Fe(II)s model presented in this paper is in accordance with all previous experimental observations: (1) it is in accord with all the data supporting the Fe′ model, since the unchelated Fe is the principal substrate for reduction and uptake in media where Fe′ is buffered by an excess of chelating agent such as EDTA; (2) it is also in accord with laboratory and field observations of diatom uptake of siderophore-bound Fe, through extracellular reduction of the complex prior to the Fe acquisition. Using the specific Fe(II) ligand FZ, we have shown that Fe(III) reduction is proportional to Fe′ in EDTA-buffered medium and that binding of Fe(II) by FZ inhibits uptake. In ''blown buffer'' experiments, we have confirmed that the maximum rate of uptake in the presence of excess EDTA is determined by the rate of dissociation of FeEDTA. Finally we have demonstrated that high concentrations of any ligand capable of binding Fe(II) (including EDTA and DFB, as well as FZ and BPDS) can inhibit uptake through a mechanism independent of any effect on Fe speciation in the bulk medium. Such inhibition implies that Fe uptake is a multistep process and is fully in accord with the notion that extracellular Fe reduction must occur before transport into the cell.

The Fe(II)s model provides a convenient framework for designing and interpreting Fe uptake experiments in a variety of natural and artificial media. The strength of the model lies in its flexibility and simplicity. It is completely specified by adjusting only three parameters—$k_{red}^{Fe(III)'}$, k_{red}^{FeY}, and k_z/k_{up}—and in most cases only one or two of these parameters are actually important. In the absence of a large excess of chelating agent or a specific Fe(II) chelating agent to bind the Fe(II) formed at the surface, k_z/k_{up} can be ignored. In many cases the reduction of Fe(III)′ will dominate over that of FeY (and k_{red}^{FeY} can be ignored) or, vice versa, the reduction of FeY will dominate (and $k_{red}^{Fe(III)'}$ can be ignored).

As described here, the Fe(II)s model is clearly incomplete. It is formulated to describe the kinetics of a nonsaturated uptake system in which the activities of the enzymes involved in Fe uptake (e.g., reductase, oxidase, and permease) increase linearly with the concentrations of their respective substrates. These conditions are applicable to most oceanographic settings and to laboratory cultures growing under Fe limitation. The model could be readily extended to account for saturation of the uptake system by replacing the first-order kinetics expression with Michaelis-Menten kinetics. (The resulting equations would of course be more complicated.) More importantly, the Fe(II)s model is not mechanistic, it does not purport to represent or take into account all individual molecular steps involved in uptake. As a result, caution should be exercised not to overstretch some of the model predictions. For example, we do not know how Fe(III) in FeY is reduced, released from the complex, and transferred to the transporter. The intermediate Fe(II) at the sur-

face is presumably bound at all times by surface ligands and not likely to be released back to the medium at significant rates (in the absence of excess Fe(II) chelator), by cells that are Fe starved. We know that Fe(II) at the surface is accessible to some ligands in the medium, but since we have no information on its coordination, we cannot predict precisely how various ligands will interfere with uptake. For example, we found that 300 μmol L^{-1} FZ had no effect on the rate of FeDFB uptake, while similar concentrations of BPDS significantly inhibited uptake. We presume that this difference between FZ and BPDS reflects different abilities to form ternary Fe(II) complexes at the surface of the cells. As mentioned before, the inhibitory effect of FZ on uptake in several of our experiments was larger than could be accounted for by FZ binding of Fe(II), and we presume that it may result from the formation of a slowly reacting ternary complex at the surface.

The Fe(II)s model provides some new insights into field and laboratory data showing inhibition of Fe uptake by DFB. DFB has been used in several studies to manipulate the availability of Fe (Wells et al. 1994; Hutchins et al. 1999*a*; Wells and Trick 2004). In many field experiments, for example, DFB was added at high concentrations (10–100 nmol L^{-1}) with the idea to favor complete exchange of Fe from its natural complexes to DFB (Wells 1999; Eldridge et al. 2004). Such DFB additions were found to strongly inhibit iron uptake and phytoplankton growth in offshore and near shore waters. According to the Fe(II)s model, however, the inhibitory effect of DFB (especially at high concentrations) on microorganism growth may result not only from its induced change in Fe speciation, but also from its ability to compete with the cells for Fe(II)s. For example, we were able to model the results of laboratory experiments showing a decrease in Fe uptake by *T. oceanica* from FeDFB with increasing DFB concentrations (between 0.1 and 10 μmol L^{-1} DFB, at 10 nmol L^{-1} Fe) (Maldonado et al. 2001). According to the Fe(II)s model, addition of DFB in a system buffered by FeDFB should not affect the ''availability'' of Fe (which depends only on the reduction of FeDFB) but should inhibit uptake through competition with the cells for Fe(II)s (Table 1).

For understanding the pathways of Fe acquisition by phytoplankton in natural waters, it would be most useful to be able to compare the reduction rate constants, k_{red}^{FeY} of different phytoplankton species for different FeY complexes (Table 1). The values of k_{red}^{FeDFB} calculated from the data of Maldonado and Price (2001) for *T. oceanica* are in reasonable agreement with our values, while the values calculated from the data of Hutchins et al. (1999*b*) for *T. weissflogii* are somewhat higher (Table 1). Our preliminary estimation of Fe-EDTA reduction is very imprecise, but it implies that Fe-EDTA reduction by *T. weissflogii* is at least 10 times slower than FeDFB reduction. Conversely, Hutchins et al. (1999*b*) found small differences in rates of uptake from various Fe complexes, such as ferrioxamine, ferrichrome, alterobactin A and B, and phaeophytin (from 8×10^{-19} to 3×10^{-18} mol $cell^{-1}$ h^{-1}), implying that, according to the Fe(II)s model, the corresponding reduction constants for the different complexes (8.3×10^{-11} to 1.9×10^{-10} L $cell^{-1}$ h^{-1}; Table 1) are fairly similar.

All available data indicate that the rate of uptake of unchelated Fe by phytoplankton is much faster (about a thousand times faster) than the rate of uptake Fe from Fe chelates (Table 1). As has been noted before (e.g., Sunda and Huntsman 1995; Price and Morel 1998), this result suggests that processes that momentarily increase Fe′ in seawater, e.g., photoreductive dissolution of Fe oxides (Waite and Morel 1984; Miller et al. 1995) and photodegradation of Fe chelates (Barbeau et al. 2001; Powell and Wilson-Finelli 2003), may be important for augmenting the Fe supply to phytoplankton. In the absence of firm information to quantify such dynamic processes, we can make a rough calculation of the relative ''availability'' of the various forms of Fe, based on published concentration and speciation data. The Fe(III)′ concentration in the open ocean ($\sim$0.07 pmol L^{-1}, Rue and Bruland 1997) has been reported to be three orders of magnitude lower than total dissolved Fe concentrations ($\sim$70 pmol L^{-1}, Johnson et al. 1997). We take arbitrarily the average of the upper range of our reduction rate constants for Fe(III)′ and FeY (not including FeEDTA) in Table 1 to represent the Fe physiology of open ocean phytoplankton: $k_{red}^{FeY} \sim 8 \times 10^{-11}$ L $cell^{-1}$ h^{-1}, $k_{red}^{Fe(III)'} \sim 4 \times 10^{-8}$ L $cell^{-1}$ h^{-1}. The resulting Fe supply rate of 2×10^{-19} mol Fe $cell^{-1}$ d^{-1} is within the range of estimated oceanic phytoplankton requirement of 2×10^{-20} to 4×10^{-18} mol Fe $cell^{-1}$ d^{-1} (assuming requirement of 2–4 pmol L^{-1} d^{-1} and 10^6 to 10^8 cell L^{-1}). According to the calculation, Fe would be contributed two-thirds by FeY and one-third by Fe(III)′.

A more general examination of the relative roles of chelated and unchelated Fe in the nutrition of phytoplankton is obtained by examining the uptake equations (Eqs. 4 and 5). If we consider the conditions where no external ligand competes effectively with the cells for Fe(II) at the surface (C is small) and the cell concentration is too small to ''blow'' the buffer ($k_{red}^{Fe(III)'}N$ is small), the uptake rate simplifies to

$$\text{uptake } (\rho) = \left(k_{red}^{FeY} + \frac{k_{red}^{Fe[III]'} k_d}{k_f [Y]}\right)[FeY] \qquad (9)$$

The predominance of Fe(III)′ or FeY in supplying Fe to the cell will be determined by the relative values of the first and second term. These are equal (taking the logs) when

$$\log Y = \log k_{red}^{Fe(III)'} - \log k_{red}^{FeY} - \log K \qquad (10)$$

where $K = k_f/k_d$ is the effective equilibrium constant for the formation of FeY. This equation provides a dividing line in a graph of log K versus log [Y]. This dividing line is plotted on Fig. 7 using $k_{red}^{Fe(III)'} = 1 \times 10^{-8}$ L $cell^{-1}$ h^{-1} and a range of values for k_{red}^{FeY} from 1×10^{-10} L $cell^{-1}$ h^{-1} to 1×10^{-12} L $cell^{-1}$ h^{-1} (Table 1, Fig. 7). Strong ligands at high concentrations plot in the upper right corner of the graph, where uptake is predicted to occur via FeY reduction. Weak ligands at low concentrations plot in the lower left corner of the graph, where uptake is predicted to proceed via Fe(III)′ reduction. The exact position of the dividing line is given by the ratio $k_{red}^{Fe(III)'}/k_{red}^{FeY}$, which depends on the nature of the ligand Y and the physiological properties of the phytoplankton species. We see that the direct reduction of FeDFB (represented by points on the right side of the graph) indeed supplies Fe to the cells at all concentrations used in uptake

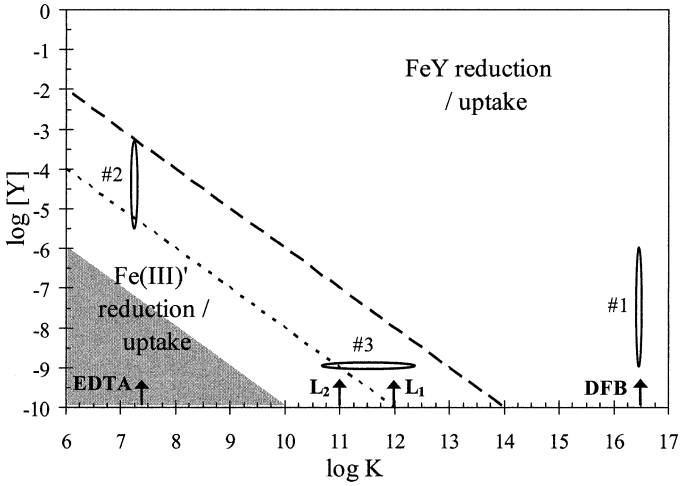

Fig. 7. The predominance of Fe(III)′ or FeY in supplying Fe to the cell is determined by the concentration of ligand (Y) (in excess of Fe) and its conditional stability constant (K) (*see text and Eqs. 9 and 10*). Strong ligands at high concentrations plot in the upper right corner of the graph, where uptake is predicted to occur via FeY reduction. Weak ligands at low concentrations plot in the lower left corner of the graph, where uptake is predicted to proceed via Fe(III)′ reduction. The dividing zone between these areas, from $k_{red}^{FeY} = 1 \times 10^{-12}$ L cell^{-1} h^{-1} (dashed line) to $k_{red}^{FeY} = 1 \times 10^{-10}$ L cell^{-1} h^{-1} (dotted line), plotted using Eq. 10 and $k_{red}^{Fe(III)'} = 1 \times 10^{-8}$ L cell^{-1} h^{-1}, represents equal contribution of Fe(III)′ and FeY uptake. Conditional stability constants for EDTA, DFB, and averages of the major classes of ligands in the ocean (L_1 and L_2) are marked by arrows. The concentrations of free DFB and EDTA commonly applied in uptake experiments are marked by ellipses 1 and 2, respectively. An approximate concentration of free ligands present in the ocean is marked by ellipse 3. The gray corner is an area where $[Y] < 1/K$ and hence Fe is not buffered by Y.

experiments (ellipse 1, Fig. 7). Conversely, Fe(III)′ (represented by points on the left side of the graph) is the dominant source of Fe in EDTA-buffered systems under most experimental conditions (ellipse 2, Fig. 7). The two ligand classes L_1 and L_2 that have been detected at concentrations of ~0.5 and 1.5 nmol L^{-1}, respectively, in the oceans (e.g., Gledhill and van Den Berg 1994; Rue and Bruland 1995; Wu and Luther 1995) are represented by ellipse 3, which is nearly in the center of the graph and straddles our choice of dividing lines. Thus such ligands may provide Fe to marine phytoplankton both through dissociation and buffering of Fe′ and through direct reduction at the cell surface. The challenge clearly is to further characterize these ligands and their abilities to supply Fe to marine microorganisms.

References

ALLNUTT, F. C. T., AND W. D. J. BONNER. 1987*a*. Evolution of reductive release as mechanism for iron uptake from ferrioxamine B by *Chlorella vulgaris.* Plant Physiol. **85:** 751–756.

——— AND ———. 1987*b*. Characterization of iron uptake from ferrioxamine B by *Chlorella vulgaris.* Plant Physiol. **85:** 746–750.

ANDERSON, M. A., AND F. M. M. MOREL. 1980. Uptake of Fe(II) by a diatom in oxic culture medium. Mar. Biol. Lett. **1:** 263–268.

——— AND ———. 1982. The influence of aqueous iron chemistry on the uptake of iron by the coastal diatom *Thalassiosira weissflogii.* Limnol. Oceanogr. **27:** 789–813.

———, ———, AND R. R. L. GUILLARD. 1978. Growth limitation of a coastal diatom by low zinc ion activity. Nature **276:** 70–71.

ARMBRUST, E. V., AND OTHERS. 2004. The genome of the diatom *Thalassiosira pseudonana:* Ecology, evolution, and metabolism. Science **306:** 79–86.

ASKWITH, C., AND J. KAPLAN. 1997. An oxidase-permease-based iron transport system in *Schizosaccharomyces pombe* and its expression in *Saccharomyces cerevisiae.* J. Biol. Chem. **272:** 401–405.

BARBEAU, K., E. L. RUE, K. W. BRULAND, AND A. BUTLER. 2001. Photochemical cycling of iron in the surface ocean mediated by microbial iron(III)-binding ligands. Nature **413:** 409–413.

BEINFAIT, F. 1987. Biochemical basis for iron efficiency reactions in plants. *In* G. Winkelmann, D. Van der Helm, and J. B. Neilands [eds.], Iron transport and storage in microorganisms, plants and animals. VCH Verlagsgesellschaft.

BRAND, L. E., W. G. SUNDA, AND R. R. L. GUILLARD. 1983. Limitation of marine phytoplankton reproductive rates by zinc manganese and iron. Limnol. Oceanogr. **28:** 1182–1198.

EIDE, D. J. 1998. The molecular biology of metal ion transport in *Saccharomyces cerevisiae.* Annu. Rev. Nutr. **18:** 441–469.

ELDRIDGE, M. L., AND OTHERS. 2004. Phytoplankton community response to a manipulation of bioavailable iron in HNLC waters of the subtropical Pacific Ocean. Aquat. Microb. Ecol. **35:** 79–91.

GLEDHILL, M., AND C. M. G. VAN DEN BERG. 1994. Determination of complexation of iron(III) with natural organic complexing ligands in seawater using cathodic stripping voltammetry. Mar. Chem. **47:** 41–54.

HUDSON, R. J. M., D. T. COVAULT, AND F. M. M. MOREL. 1992. Investigations of iron coordination and redox reactions in seawater using iron-59 radiometry and ion-pair solvent extraction of amphiphilic iron complexes. Mar. Chem. **38:** 209–235.

———, AND F. M. M. MOREL. 1989. Distinguishing between extracellular and intracellular iron in marine phytoplankton. Limnol. Oceanogr. **34:** 1113–1120.

——— AND ———. 1990. Iron transport in marine phytoplankton: Kinetics of cellular and medium coordination reactions. Limnol. Oceanogr. **35:** 1002–1020.

——— AND ———. 1993. Trace metal transport by marine microorganisms: Implications of metal coordination kinetics. Deep Sea Res. I **40:** 129–150.

HUTCHINS, D. A., V. M. FRANK, AND K. W. BRULAND. 1999*a*. Inducing phytoplankton iron limitation in iron-replete coastal water with a strong chelating ligand. Limnol. Oceanogr. **44:** 1009–1018.

———, A. E. WITTER, A. BUTLER, AND G. W. LUTHER. 1999*b*. Competition among marine phytoplankton for different chelated iron speciation. Nature **400:** 858–861.

JOHNSON, K. S., R. M. GORDON, AND K. H. COALE. 1997. What controls dissolved iron concentrations in the world ocean? Mar. Chem. **57:** 137–161.

JONES, G. J., B. P. PALENIK, AND F. M. M. MOREL. 1987. Trace metal reduction by phytoplankton: The role of plasmalemma redox enzymes. J. Phycol. **23:** 237–244.

KESHTACHER, L. E., Y. HADAR, AND Y. CHEN. 1999. Fe nutrition demand and utilization by the green alga *Dunaliella bardawil.* Plant Soil **215:** 175–182.

KUSTKA, A. B., Y. SHAKED, A. J. MILLIGAN, D. W. KING, AND F. M. M. MOREL. In press. Extracellular production of superoxide by marine diatoms: Contrasting implications for iron redox chemistry and bioavailability. Limnol. Oceanogr.

MALDONADO, M. T., AND N. M. PRICE. 1996. Influence of N substrate on Fe requirements of marine centric diatoms. Mar. Ecol. Prog. Ser. **141:** 161–172.

——— AND ———. 2000. Nitrate regulation of Fe reduction and transport in Fe limited *Thalassiosira oceanica.* Limnol. Oceanogr. **45:** 814–826.

——— AND ———. 2001. Reduction and transport of organically bound iron by *Thalassiosira oceanica* (Bacillariophyceae). J. Phycol. **2:** 298–309.

———, AND OTHERS. 2001. Iron uptake and physiological response of phytoplankton during a mesoscale Southern Ocean iron enrichment. Limnol. Oceanogr. **46:** 1802–1808.

MILLER, W. L., D. W. KING, J. LIN, AND D. R. KESTER. 1995. Photochemical redox cycling of iron in coastal seawater. Mar. Chem. **50:** 63–77.

MOREL, F. M. M., AND J. G. HERING. 1993. Principles and applications of aquatic chemistry. Wiley.

POWELL, R. T., AND A. WILSON-FINELLI. 2003. Photochemical degradation of organic iron complexing ligands in seawater. Aquat. Sci. **65:** 367–374.

PRICE, N. M., G. I. HARRISON, J. G. HERING, R. J. M. HUDSON, P. M. V. NIREL, B. P. PALENIK, AND F. M. M. MOREL. 1988/89. Preparation and chemistry of the artificial algal culture medium Aquil. Biol. Oceanogr. **6:** 443–461.

———, AND F. M. M. MOREL. 1998. Biological cycling of Fe in the Ocean, p. 1–36. *In* A. Sigel and H. Sigel [eds.], Metal ions in biological systems, Vol. 35. Marcel Dekker.

RUE, E. L., AND K. W. BRULAND. 1995. Complexation of iron(III) by natural organic ligands in the central North Pacific as determined by a new competitive ligand equilibration/adsorptive cathodic stripping voltammetric method. Mar. Chem. **50:** 117–138.

——— AND ———. 1997. The role of organic complexation on ambient iron chemistry in the equatorial Pacific Ocean and the response of a mesoscale iron addition experiment. Limnol. Oceanogr. **42:** 901–910.

SHAKED, Y., Y. EREL, AND A. SUKENIK. 2002. Phytoplankton-mediated redox cycle of iron in the epilimnion of Lake Kinneret. Environ. Sci. Technol. **36:** 460–467.

———, A. B. KUSTKA, F. M. M. MOREL, AND Y. EREL. 2004. Simultaneous determination of iron reduction and uptake by phytoplankton. Limnol. Oceanogr. Methods **2:** 137–145.

SORIA-DENGG, S., AND U. HORSTMANN. 1995. Ferrioxamine B and E as iron sources for the marine diatom *Phaeodactylum tricornutum*. Mar. Ecol. Prog. Ser. **125:** 269–277.

SUNDA, W. G., AND R. R. L. GUILLARD. 1976. Relationship between cupric ion activity and toxicity of copper to phytoplankton. J. Mar. Res. **34:** 511–529.

———, AND S. A. HUNTSMAN. 1995. Iron uptake and growth limitation in oceanic and coastal phytoplankton. Mar. Chem. **50:** 189–206.

———, AND ———. 1997. Interrelated influence of iron, light and cell size on marine phytoplankton growth. Nature **390:** 389–392.

———, AND ———. 2003. Effect of pH, light, and temperature on Fe-EDTA chelation and Fe hydrolysis in seawater. Mar. Chem. **84:** 35–47.

———, D. G. SWIFT, AND S. A. HUNTSMAN. 1991. Low iron requirements for growth in oceanic phytoplankton. Nature **351:** 55–57.

VAN HO, A., D. M. WARD, AND J. KAPLAN. 2002. Transition metal transport in yeast. Annu. Rev. Microbiol. **56:** 237–261.

WAITE, T. D., AND F. M. M. MOREL. 1984. Photoreductive dissolution of colloidal iron oxides in natural waters. Environ. Sci. Technol. **18:** 860–868.

WELLS, M. L. 1999. Manipulating iron availability in nearshore waters. Limnol. Oceanogr. **44:** 1002–1008.

———, N. M. PRICE, AND K. W. BRULAND. 1994. Iron limitation and the cyanobacterium Synechococcus in equatorial Pacific waters. Limnol. Oceanogr. **39:** 1481–1486.

———, AND C. G. TRICK. 2004. Controlling iron availability to phytoplankton in iron-replete coastal waters. Mar. Chem. **86:** 1–13.

WU, J., AND G. W. LUTHER III. 1995. Complexation of Fe(III) by natural organic ligands in the Northwest Atlantic Ocean by a competitive ligand equilibration method and a kinetic approach. Mar. Chem. **50:** 159–177.

Received: 12 October 2004
Accepted: 28 January 2005
Amended: 28 January 2005